Quiet-Sun Magnetism

Analysis of GREGOR/GRIS Stokes Profiles

Andreas Lagg
and the GREGOR/GRIS team[1]

Max-Planck-Institut für Sonnensystemforschung
Göttingen, Germany
[1] Kiepenheuer Institut für Sonnenphysik (KIS), Freiburg; Leibniz-Institut für Astrophysik Potsdam (AIP); Germany
Instituto de Astrofísica de Canarias (IAC), Tenerife, Spain

MAX-PLANCK-GESELLSCHAFT

SGS Seminar

MPS Göttingen

15 March 2016

MPS

Relevance

- QS magnetism covers $>$99% of solar surface (even during maxima); 15% in inter-network
- crucial to understand the solar global magnetism
- local (surface) dynamo or cascade from global dynamo?

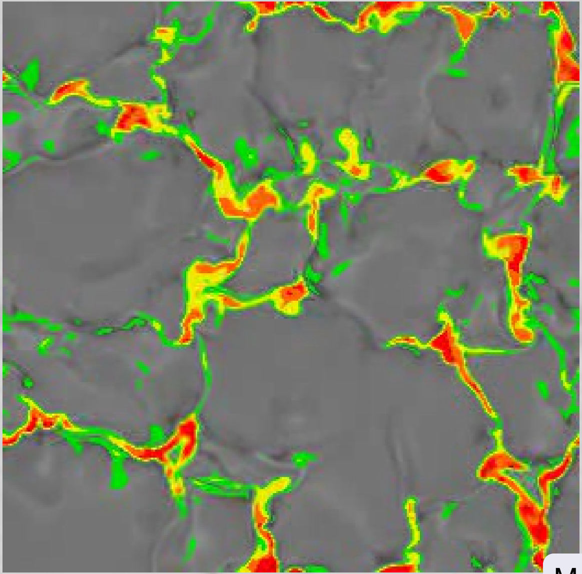

M. Rempel

Observations

Tool: spectropolarimetry (Zeeman & Hanle)

- weak signals → high sensitivity required
- small scales → high spatial resolution required

⟶ difficult measurement!

Observations

Tool: spectropolarimetry (Zeeman & Hanle)

- weak signals $\rightarrow$ high sensitivity required
- small scales $\rightarrow$ high spatial resolution required

$\longrightarrow$ difficult measurement!

The consequence

- disagreement about magnetic field strength
- disagreement about angular distribution
- disagreement about temporal behavior over activity cycle

Statistical properties: correlation with activity cycle

Hinode long-term study (Buehler et al., 2013)

- careful consideration of instrumental effects
- no cycle dependence for B_h and B_v

(also: Shchukina & Trujillo Bueno, 2003; Faurobert et al., 2001; Kleint et al., 2010)

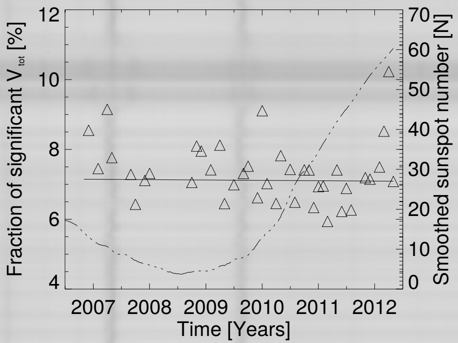

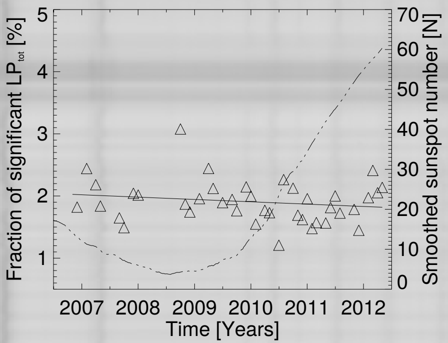

Statistical properties: correlation with activity cycle

Hinode long-term study (Buehler et al., 2013)

- careful consideration of instrumental effects
- no cycle dependence for B_h and B_v

(also: Shchukina & Trujillo Bueno, 2003; Faurobert et al., 2001; Kleint et al., 2010)

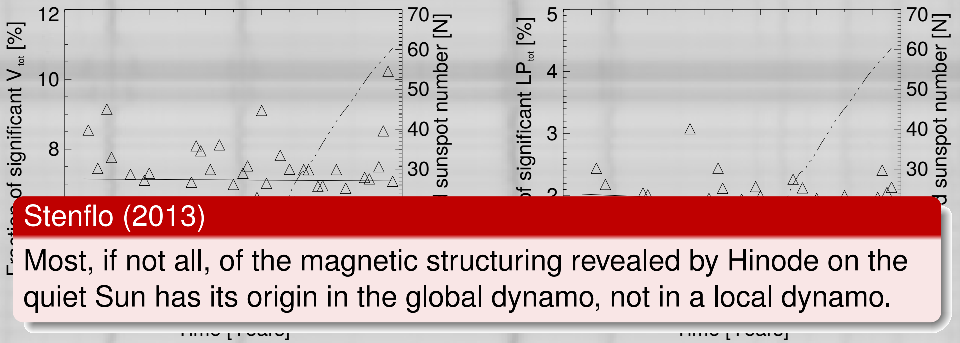

Stenflo (2013)

Most, if not all, of the magnetic structuring revealed by Hinode on the quiet Sun has its origin in the global dynamo, not in a local dynamo.

QS fields: Strength

Recent results: QS magnetic field strength (Hanle)

- Faurobert-Scholl et al. (1995): ≈30 G
- Bommier et al. (2005): 40–55 G
- Trujillo Bueno et al. (2004): 130 G
- Berdyugina & Fluri (2004): 15 G
- Asensio Ramos & Trujillo Bueno (2005): 10 G
- Shapiro et al. (2011): 40–82 G
- Kleint et al. (2010): 3-8 G (@5″)

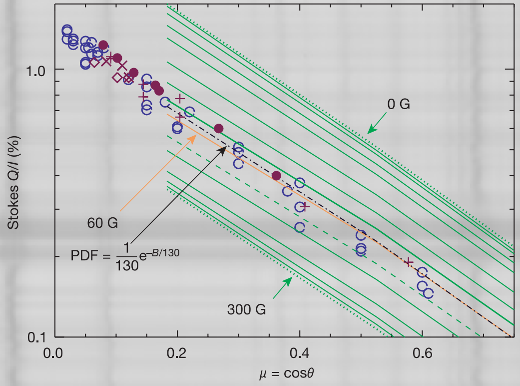

Hanle depolarization in Sr I 4607

What is the distribution of field strengths in the QS?

Same instrument: Hinode SOT/SP (Zeeman)

- Orozco Suárez et al. (2007): B_v = 9.5, B_h = 11.3
- Stenflo (2010): bimodal (B_v = 5-10; 1 kG)
- Lites et al. (2008): B_v = 11, B_h = 55
- Asensio Ramos & Martínez González (2014): < 275 G

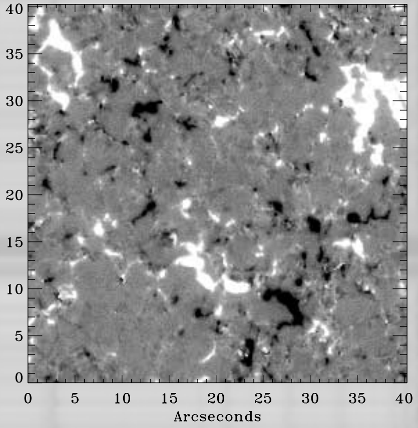

Deep mode scans Hinode SOT/SP

QS fields: Orientation

Measurements

- isotropic + horizontal peak
- isotropic
- mainly horizontal
- isotropic + vertical peak

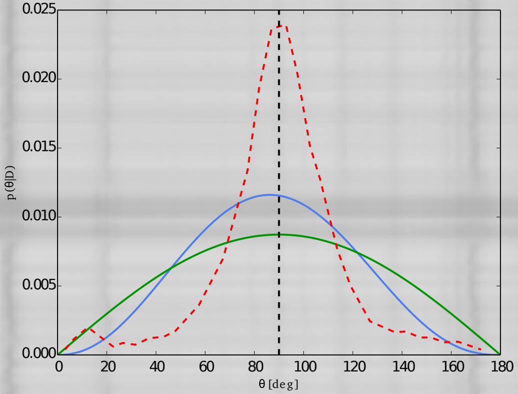

Martínez González et al. (2008); Asensio Ramos (2009); Asensio Ramos & Martínez González (2014)

Summary angular distributions (Tab. 2 from Steiner & Rezaei, 2012)

no.	authors	instrument/ simulation	line [nm]	angular distribution	$\langle B^{\mathrm{T}}_{\mathrm{app}}\rangle / \langle B^{\mathrm{L}}_{\mathrm{app}}\rangle$
1	Lites et al. (2007, 2008)	SOT/SP	630	predominantly horizontal	5
2	Orozco Suárez et al. (2007)	SOT/SP	630	predominantly horizontal	2.1
3	Martínez González et al. (2008)	VTT/TIP	1560	isotropic distribution	—
4	Beck & Rezaei (2009)	VTT/TIP	1560	predominantly vertical	0.42
5	Asensio Ramos (2009)	SOT/SP	630	isotropic for weak fields	—
6	Danilovic et al. (2010)	SOT/SP	630	predominantly horizontal	5.8
7	Stenflo (2010)	SOT/SP	630	predominantly vertical	—
8	Ishikawa & Tsuneta (2011)	SOT/SP	630	predominantly vertical	0.86
9	Borrero & Kobel (2011)	SOT/SP	630	undeterminable	—
10	Borrero & Kobel (2012)	SOT/SP	630	non-isotropic	—
11	Steiner et al. (2008)	h20	630	predominantly hor-	4.3 (2.8)
		v10	630	izontal	1.6 (1.5)
12	Danilovic et al. (2010)	C mf=3	630	predominantly hor-	9.8 (3.5)
		$C{+}B_{\mathrm{ver}}$	630	izontal	4.2 (2.6)

Summary of observations

Summary of observations

Reason 1: Sensitivity of polarimeters

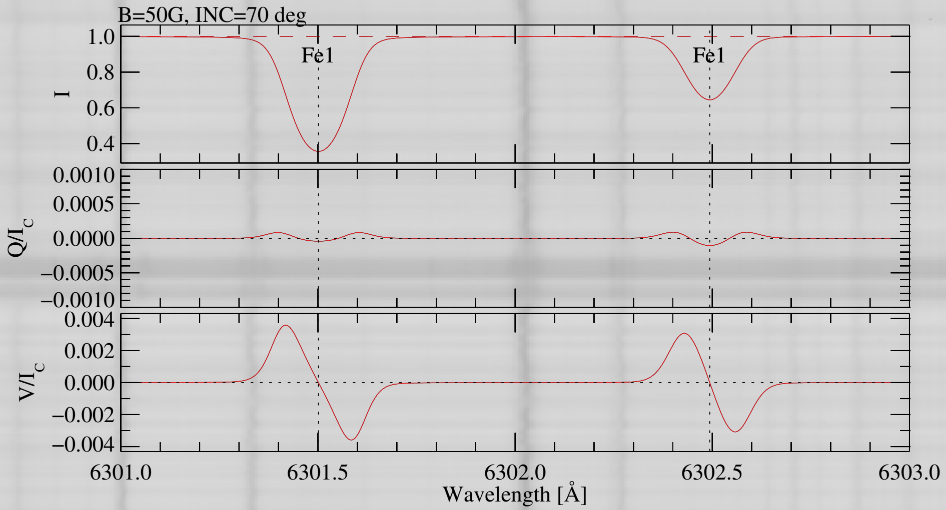

Reason 2: Bias introduced by Zeeman effect

weak-field limit

$$B_{||} \propto V$$
$$B_{\perp} \propto [Q^2 + U^2]^{1/4}$$

(w.r.t. line-of-sight)

Stenflo (2013)

- ⇒ noise leads to more horizontal fields (disk center)
- ⇒ apparent flux: 25× higher in $B_{\perp}$ non-Gaussian

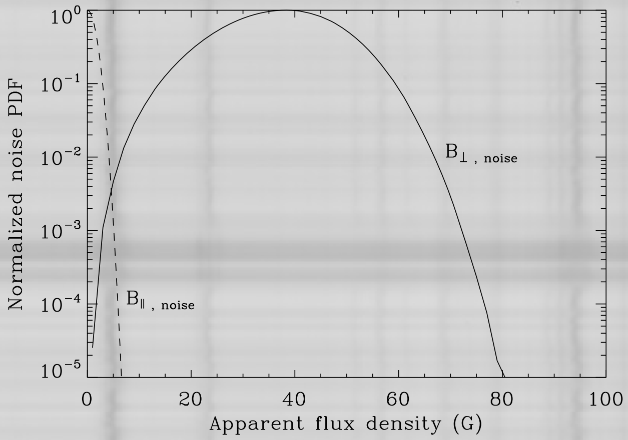

Hinode SOT/SP example

Reason 3: Height dependent B_v & B_h

B_v vs. B_h

depends strongly on

- spectral line selection
- analysis method (height dependent inversion vs. ME)
- heliocentric angle (higher opacity at limb)

small scale dynamo dynamo

- MHD: $P(\gamma) \propto \sin\gamma$ (e.g. Vögler & Schüssler, 2007)
- height dependent (Rempel, 2014)

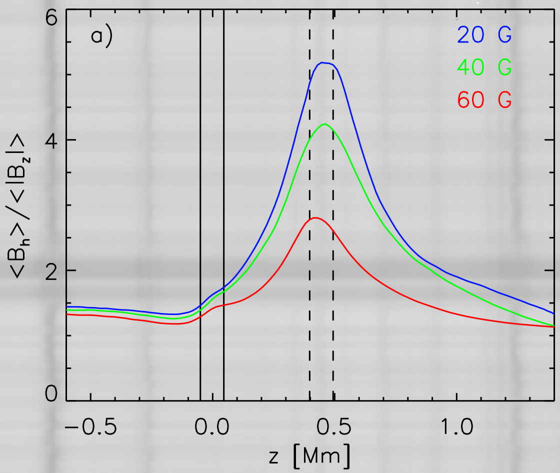

Rempel (2014)

Reason 4: Methods for QS diagnostics

Analysis methods

- Zeeman vs. Hanle
- selection of profiles (σ-level)
- inversions
  - ME vs. height dependent
  - filling factor
- direct techniques (e.g. line ratio)

Reason 5: Unresolved Stokes signals – signal cancellation

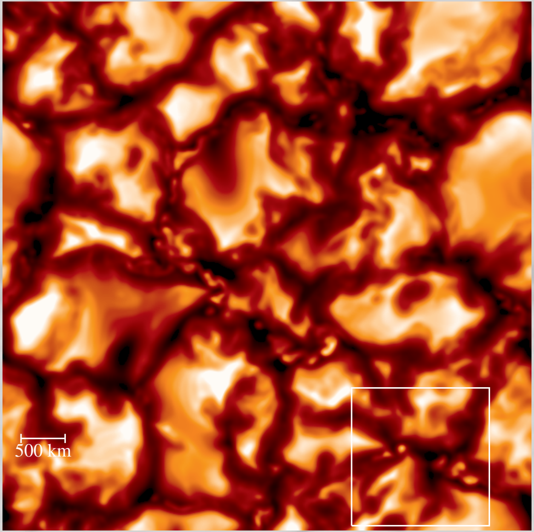

Reason 5: Unresolved Stokes signals – signal cancellation

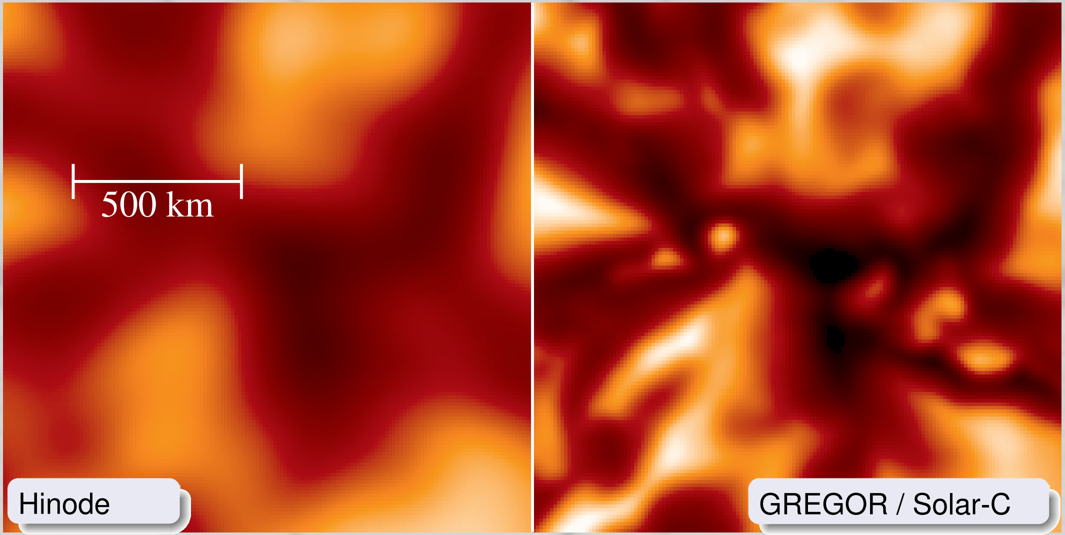

Reason 5: Unresolved Stokes signals – signal cancellation

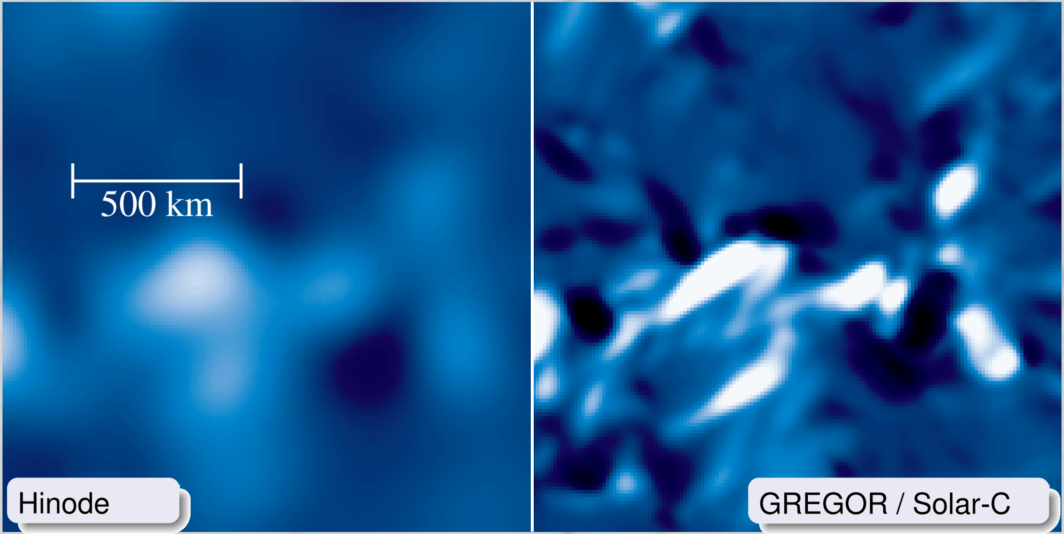

Possible solutions?

Increase spatial resolution

- larger telescope aperture

Increase signal/noise ratio

- more photons
- better polarimeter
- more sensitive spectral lines

Remove height bias

- select lines with narrow and known formation height

Remove model ambiguities

- select simple, bias-free analysis method without

Recent results from GREGOR / GRIS

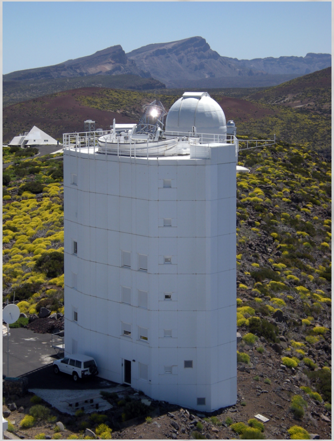

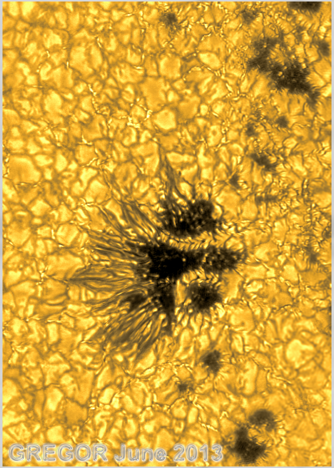

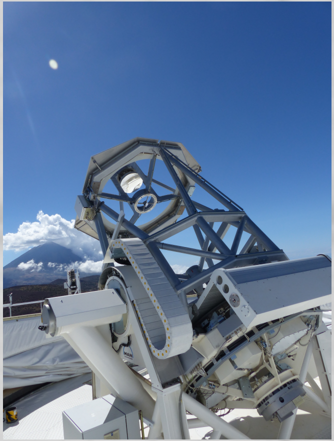

GREGOR Infrared Spectrograph (GRIS; Collados et al., 2012)

GRIS fact sheet

- WL-range 1–2.3μm
- sensitivity $< 10^{-4}$
- $\lambda/\Delta\lambda \approx$ 120 000 (@1.56 μm)
- mounted at 1.5 m GREGOR telescope
- 0.″18–0.″30 resolution

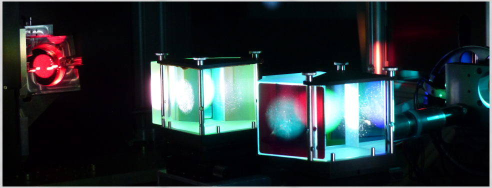

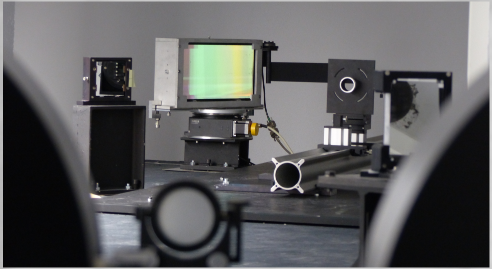

Scan of quiet sun region (2015-Sep-17)

- disk center
- exp. time: 4.8 s/slit (8 s cadence)
- noise level (unbinned): $4 \cdot 10^{-4}$ I_C
- $\lambda/\Delta\lambda \geq 120\,000$, 40 mÅ sampling
- spatial resolution: 0.″40 (diff. limit 0.″26), sampling: 0.″135

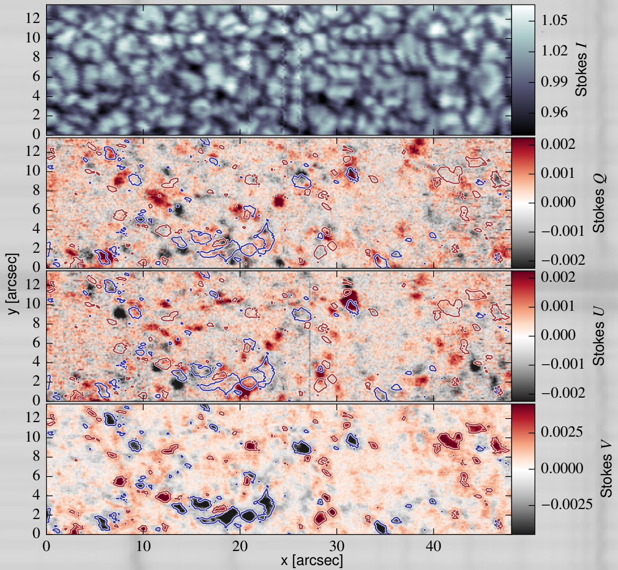

Scan of quiet sun region (2015-Sep-17)

- FFT rebinned: 0.″135 pixelsize
- → 0.″20 pixelsize
- noise level reduction: $4 \cdot 10^{-4}$ I_C
- → $2.7 \cdot 10^{-4}$ I_C
- → no loss in spatial resolution
- spectral binning
- → ×2 (oversampling)
- → $2.1 \cdot 10^{-4}$ I_C

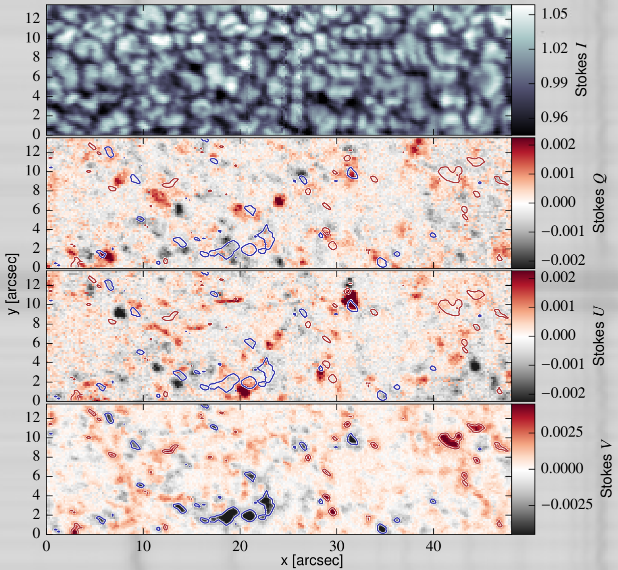

Stokes Profiles: Granule (=0.″135 pixel, noise level: $4 \cdot 10^{-4}$)

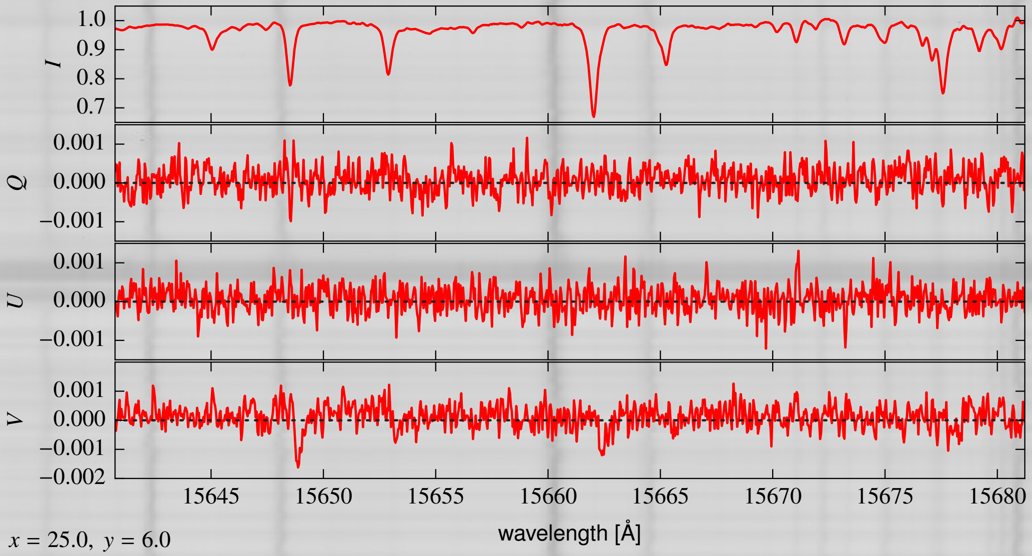

Stokes Profiles: Granule FFT binned (=0.″20 pixel, noise level: $2.7 \cdot 10^{-4}$)

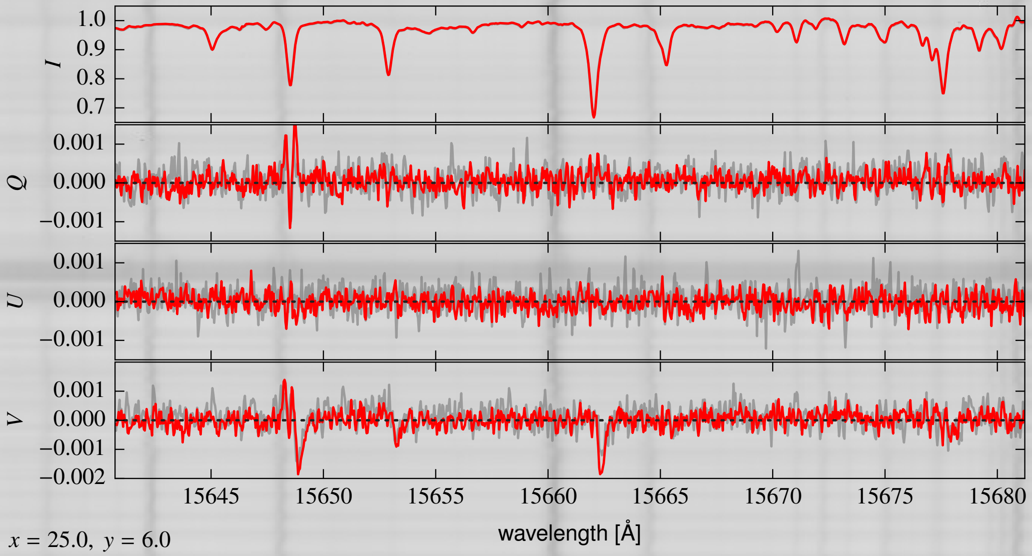

Comparison: GRIS vs. SOT/SP

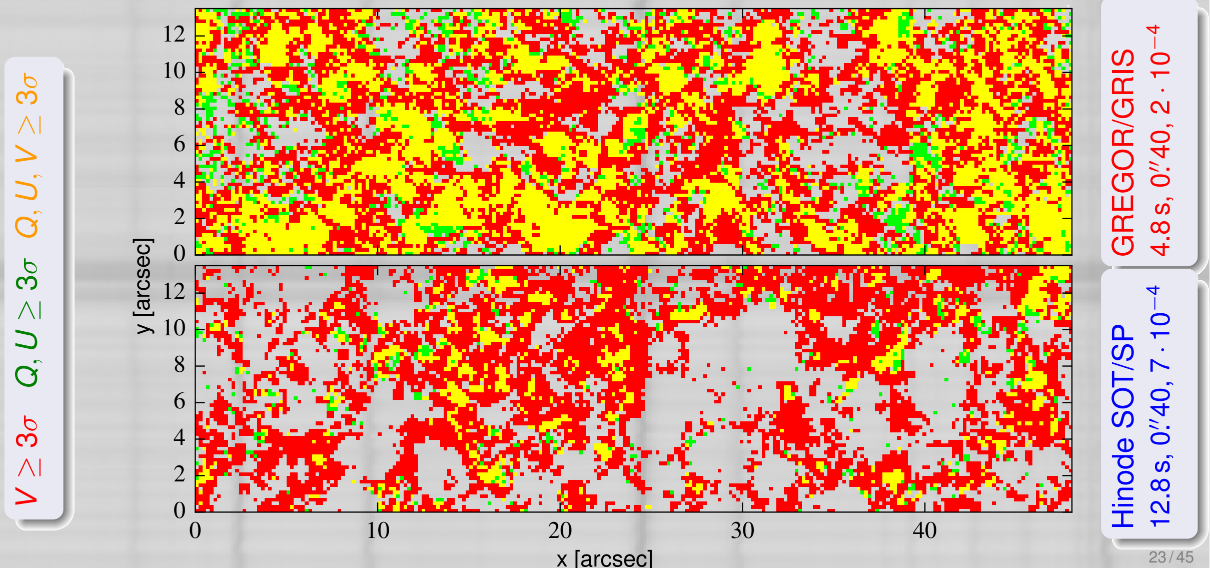

Stokes signal levels

Comparison GRIS ↔ Hinode SOT/SP

σ-level	GRIS [%] LP	CP	LP and CP	LP or CP	SOT/SP [%] LP	CP	LP and CP	LP or CP
3σ	39.7	73.0	33.1	79.7	9.8	49.3	7.7	51.4
4σ	18.4	57.0	13.9	61.5	4.2	37.1	3.1	38.2
5σ	9.2	44.2	6.2	47.2	2.1	28.5	1.5	29.1

Simple diagnostic techniques: MLR - field strength

Magnetic Line Ratio (Solanki et al., 1992)

$$\mathrm{MLR} = \frac{g_{\mathrm{eff}}(15652)\,V_{\mathrm{max}}(15648)}{g(15648)\,V_{\mathrm{max}}(15652)}$$

Requirements:

- spectral lines identical except for Landé factor
- 2 distinct components:
  (1) magnetized, (2) field-free
- small gradients in log τ

$\rightarrow$ not fulfilled for Fe I 1.56 line pair

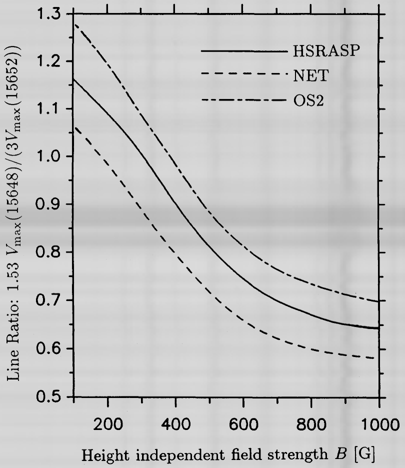

Simple diagnostic techniques: MLR - field strength

Magnetic Line Ratio (Solanki et al., 1992)

$$\mathrm{MLR} = \frac{g_{\mathrm{eff}}(15652)\,V_{\mathrm{max}}(15648)}{g(15648)\,V_{\mathrm{max}}(15652)}$$

Requirements:

- spectral lines identical except for Landé factor
- 2 distinct components:
  (1) magnetized, (2) field-free
- small gradients in $\log\tau$

$\rightarrow$ not fulfilled for Fe I 1.56 line pair

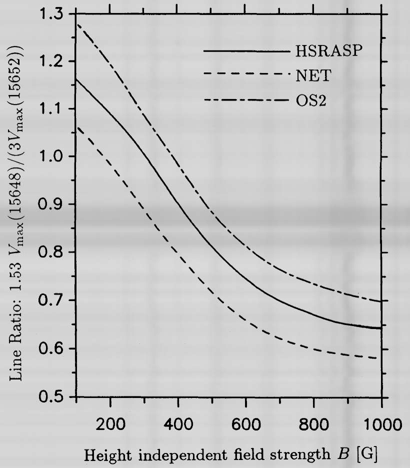

Simple diagnostic techniques: MLR - field strength

Magnetic Line Ratio (Solanki et al., 1992)

$$\mathrm{MLR} = \frac{g_{\mathrm{eff}}(15652)\, V_{\mathrm{max}}(15648)}{g(15648)\, V_{\mathrm{max}}(15652)}$$

Requirements:

- spectral lines identical except for Landé factor
- 2 distinct components:
  (1) magnetized, (2) field-free
- small gradients in $\log \tau$

→ not fulfilled for Fe I 1.56 line pair

→ BUT: similar formation height, narrow formation height range, similar thermal properties

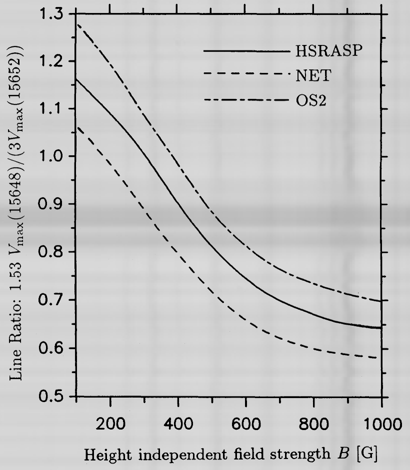

MLR analysis - select “normal” profiles

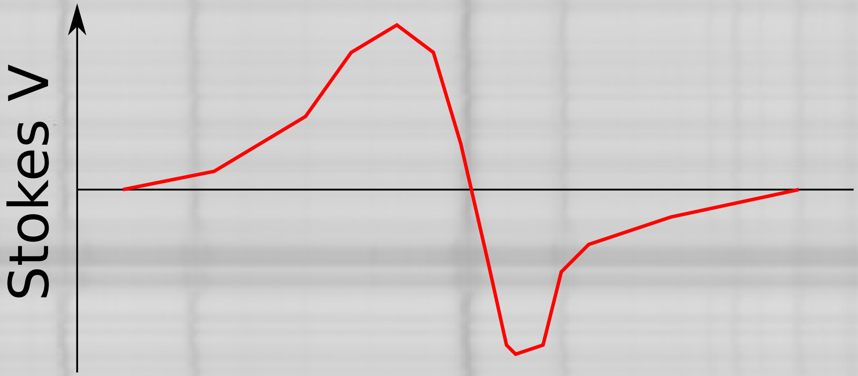

MLR analysis - select “normal” profiles

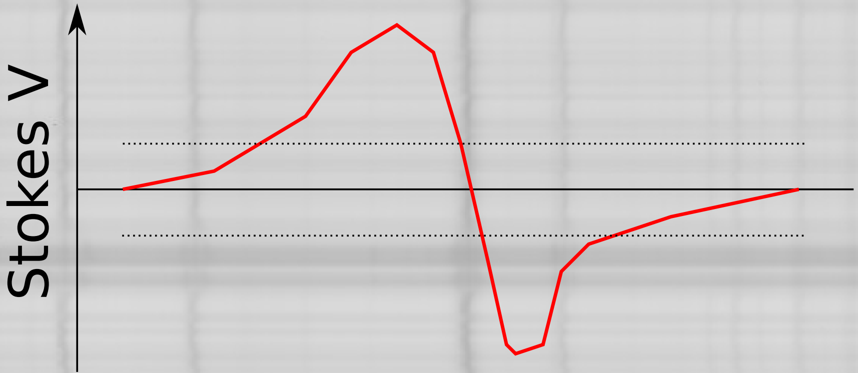

noise threshold 3σ

MLR analysis - select “normal” profiles

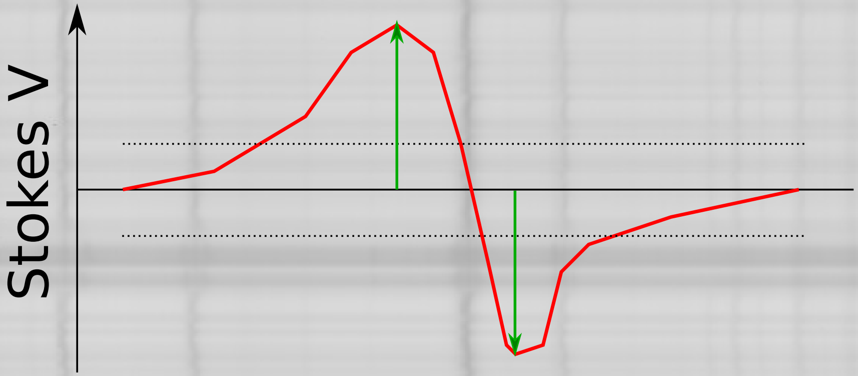

noise threshold 3σ

small amplitude asym. δa

MLR analysis - select “normal” profiles

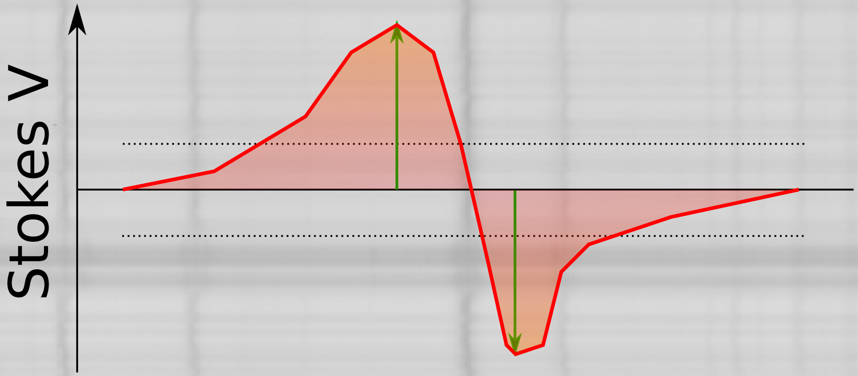

noise threshold 3σ

small amplitude asym. δa

small area asym. δA

MLR analysis - select “normal” profiles

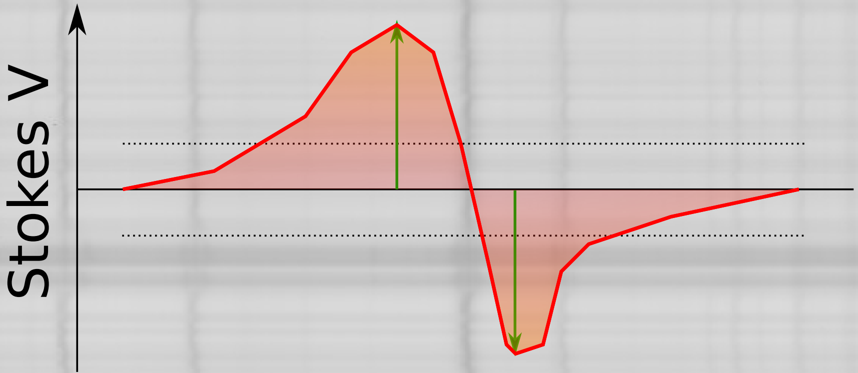

noise threshold 3σ

small amplitude asym. δa

small area asym. δA

(43.7% of the profiles)

MLR Fe I 15648 / Fe I 15652

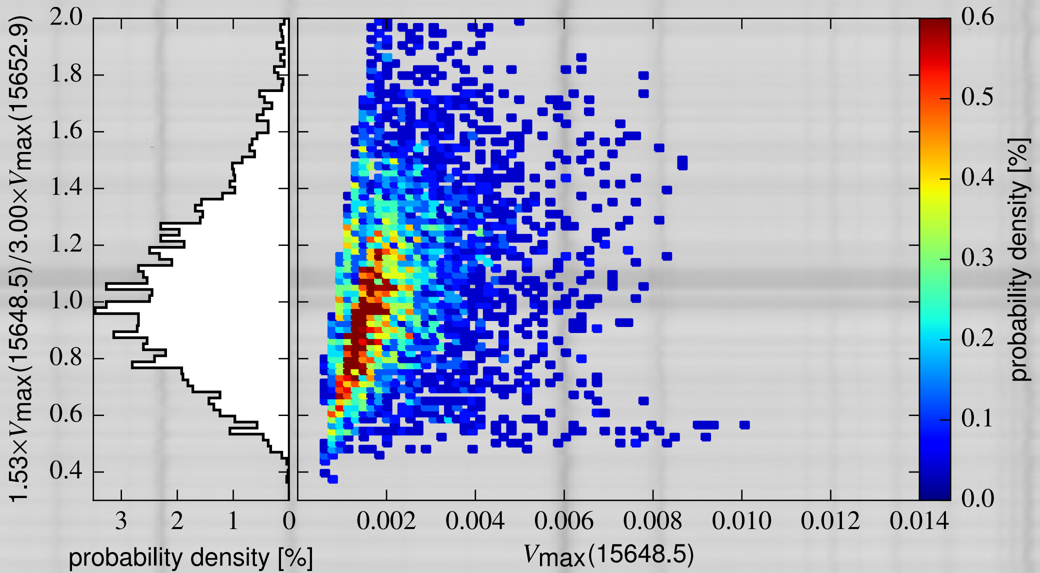

Different MLR regions

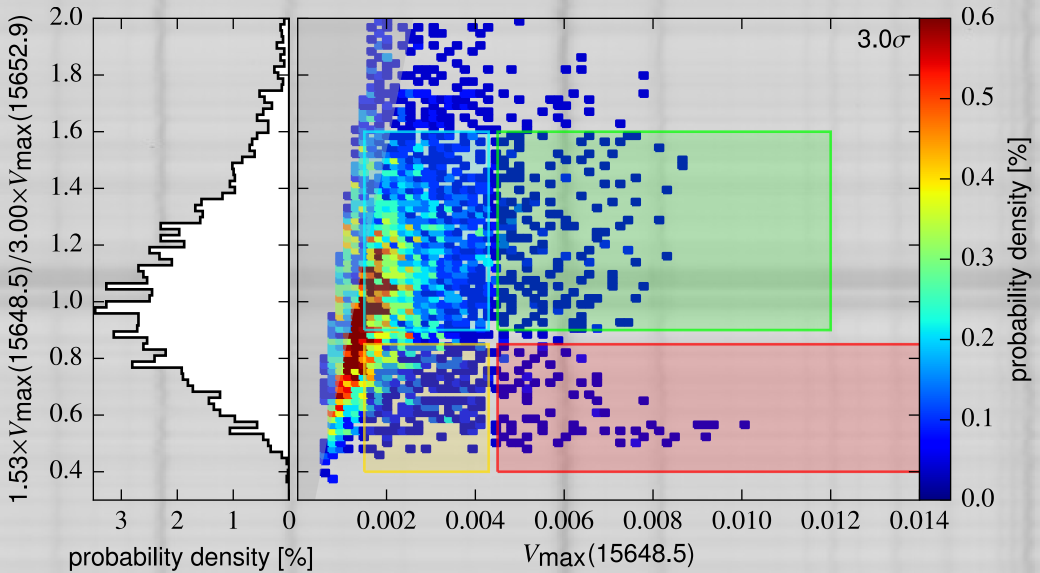

MLR: Statement about field strength possible?

Blue Region:
MLR≈1.2, small V_{max}

Green Region:
MLR≈1.2, large V_{max}

Yellow Region:
MLR≈0.6, small V_{max}

Red Region:
MLR≈0.6, large V_{max}

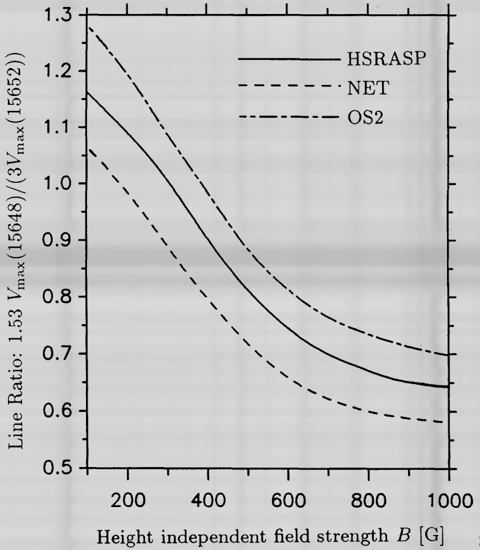

MLR: Statement about field strength possible?

<hecto-Gauss region

Blue Region:
MLR≈1.2, small V_{max}

Green Region:
MLR≈1.2, large V_{max}

Yellow Region:
MLR≈0.6, small V_{max}

Red Region:
MLR≈0.6, large V_{max}

>kilo-Gauss region

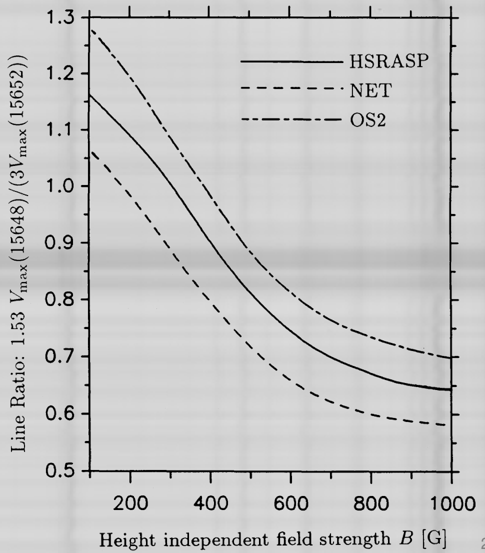

Stokes Profiles: Red: MLR≈0.6, large V_{max}, Yellow ×3: MLR≈0.6, small V_{max}

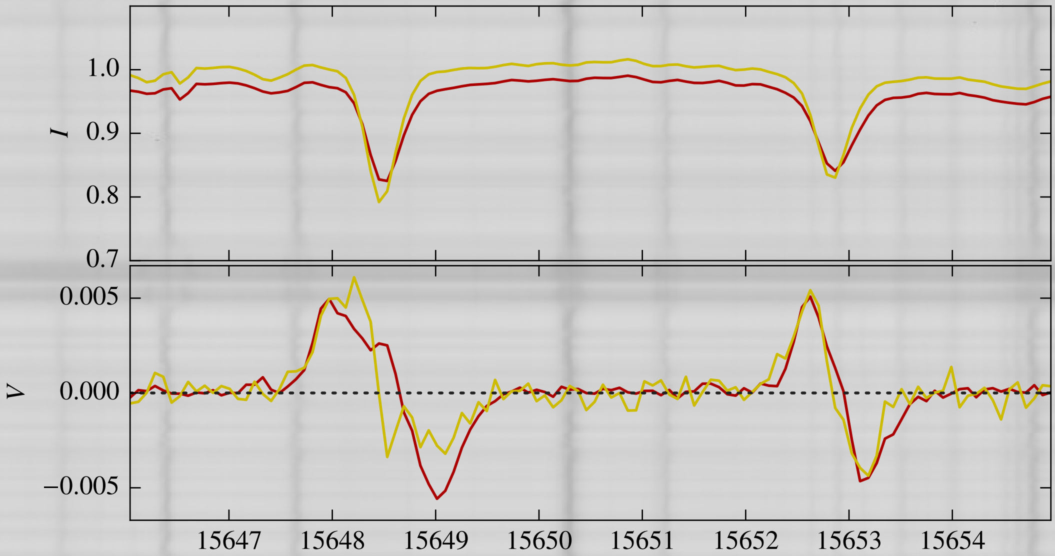

Stokes Profiles: Green: MLR≈1.2, large V_{max}, Blue ×3: MLR≈1.2, small V_{max}

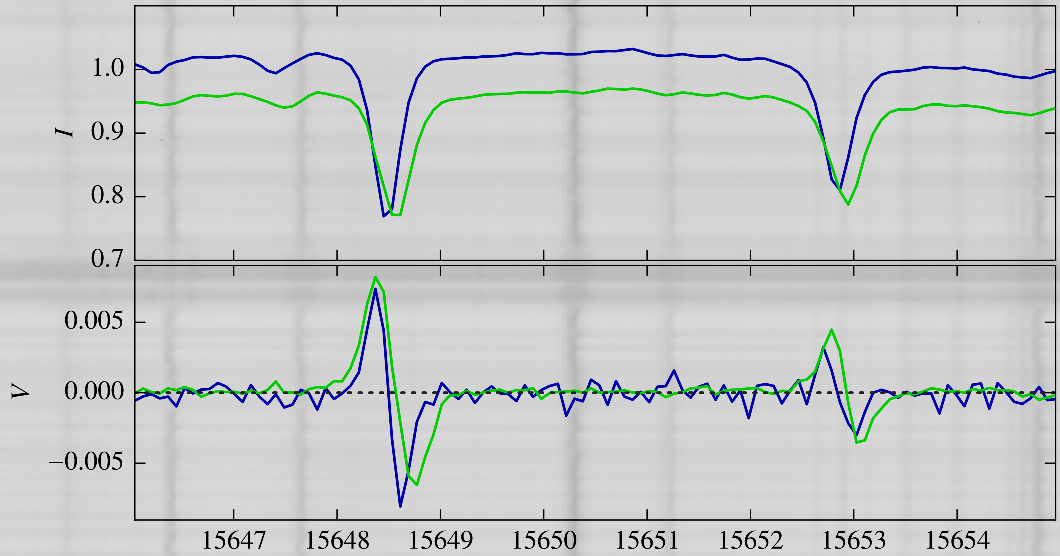

Different MLR regions - Where?

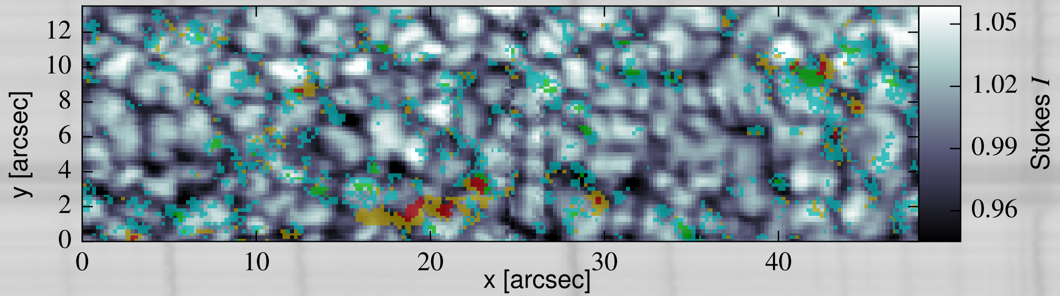

MLR≈1.2, small V_{max} (hG)

MLR≈1.2, large V_{max} (hG)

MLR≈0.6, small V_{max} (kG)

MLR≈0.6, large V_{max} (kG)

Different MLR regions - Where?

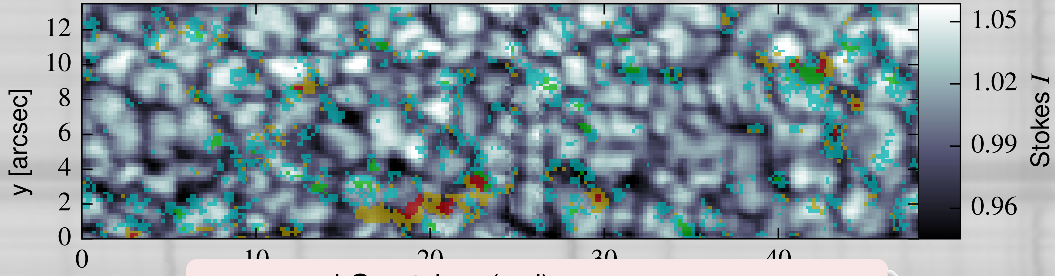

- some kG patches (red)
- surrounded by yellow halo
- ubiquitous weak fields ($\lesssim$ 500 G, green & blue)

MLR≈1.2, small V_{max} (hG) | MLR≈1.2, large V_{max} (hG) | MLR≈0.6, small V_{max} (kG) | MLR≈0.6, large V_{max} (kG)

Test using MHD Quiet Sun simulations (SSD+IMaX run)

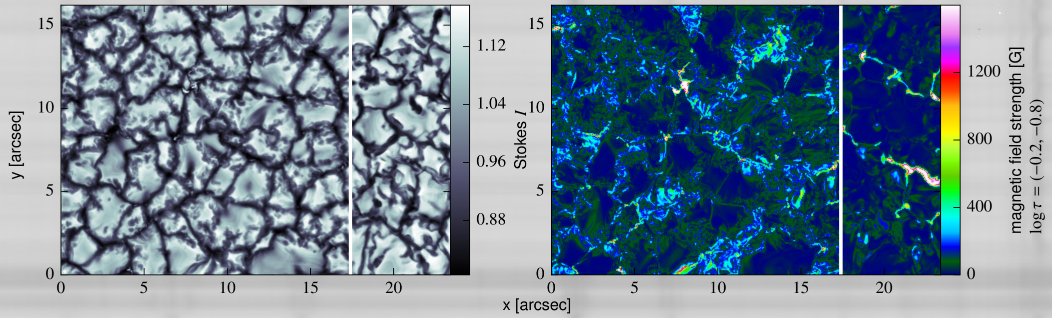

MHD simulations: SSD+IMaX run

- Rempel (2014): O16bM
- Riethmueller et al. (2016)

MLR≈1.2, small V_{max} (hG) | MLR≈1.2, large V_{max} (hG) | MLR≈0.6, small V_{max} (kG) | MLR≈0.6, large V_{max} (kG)

Test using MHD Quiet Sun simulations (SSD+IMaX run)

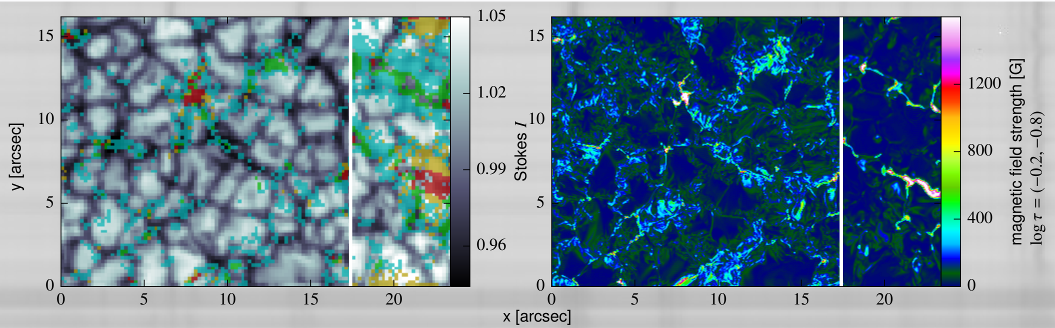

spatial degrading

- GREGOR-PSF + 0.25″ Gauss + Lorentzian wings

→ match contrast, resolution, I_c histogram

spectral degrading

- 12% straylight
- 150 mÅ Gauss

MLR≈1.2, small V_{max} (hG) | MLR≈1.2, large V_{max} (hG) | MLR≈0.6, small V_{max} (kG) | MLR≈0.6, large V_{max} (kG)

MLR (SSD + IMaX run, degraded)

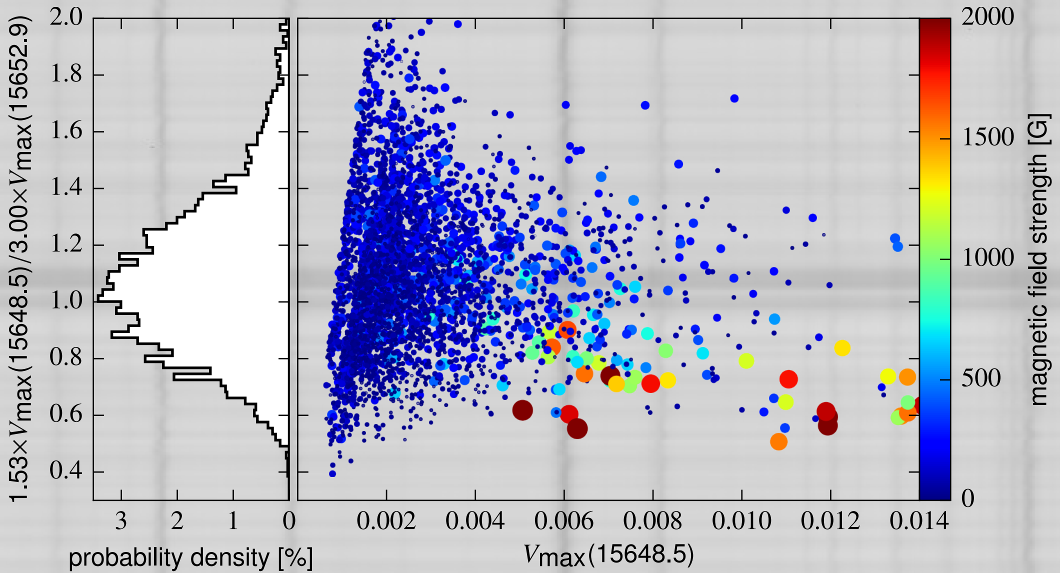

MLR (SSD + IMaX run, degraded)

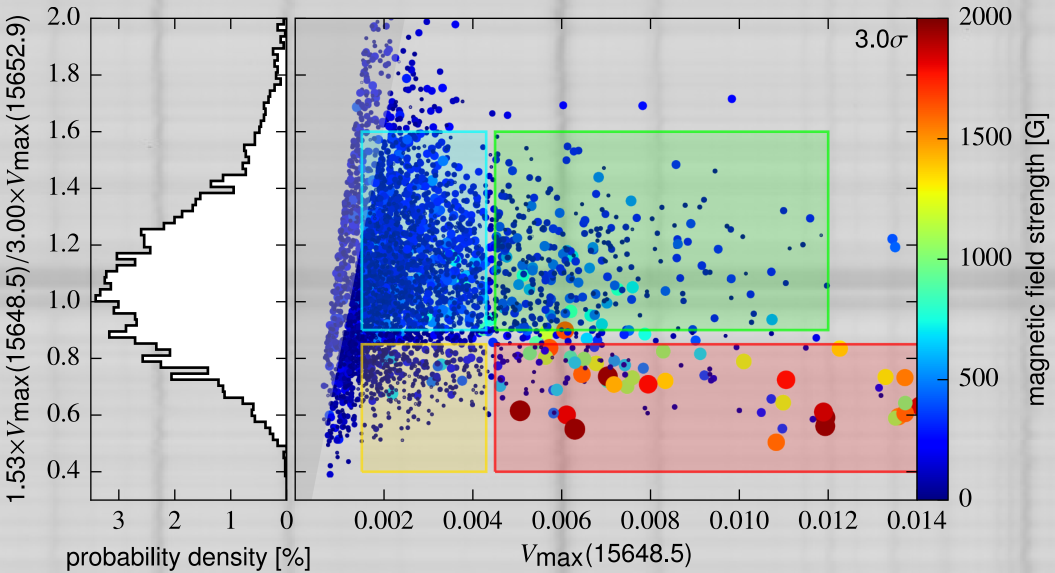

MLR (SSD + IMaX run, degraded)

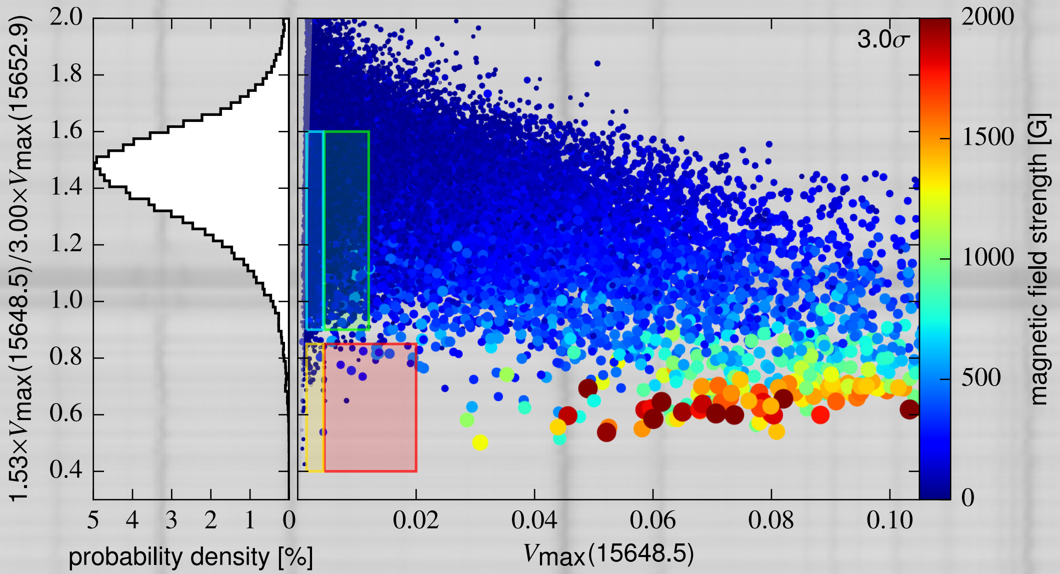

MLR (SSD + IMaX run, degraded)

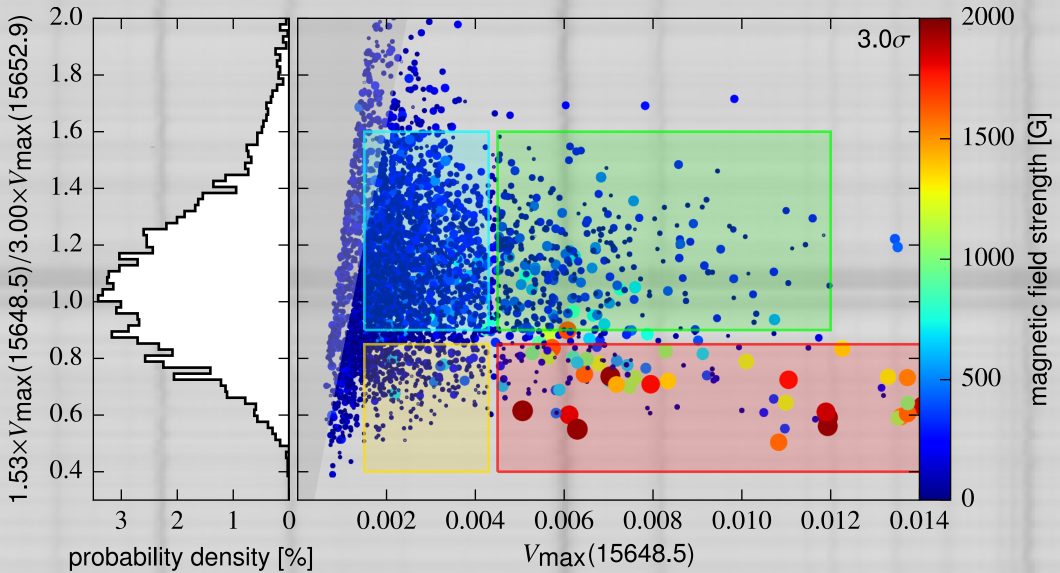

Different MLR regions - Where?

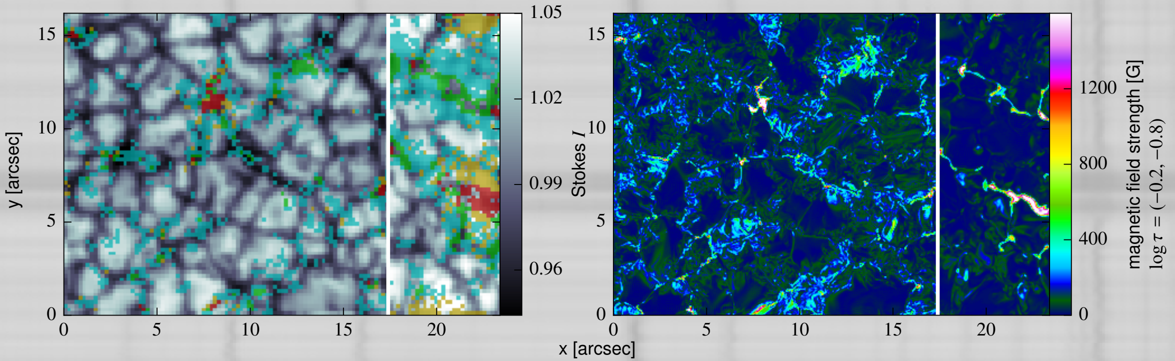

MLR≈1.2, small V_{max} (hG)

MLR≈1.2, large V_{max} (hG)

MLR≈0.6, small V_{max} (kG)

MLR≈0.6, large V_{max} (kG)

B strength (SSD + IMaX run)

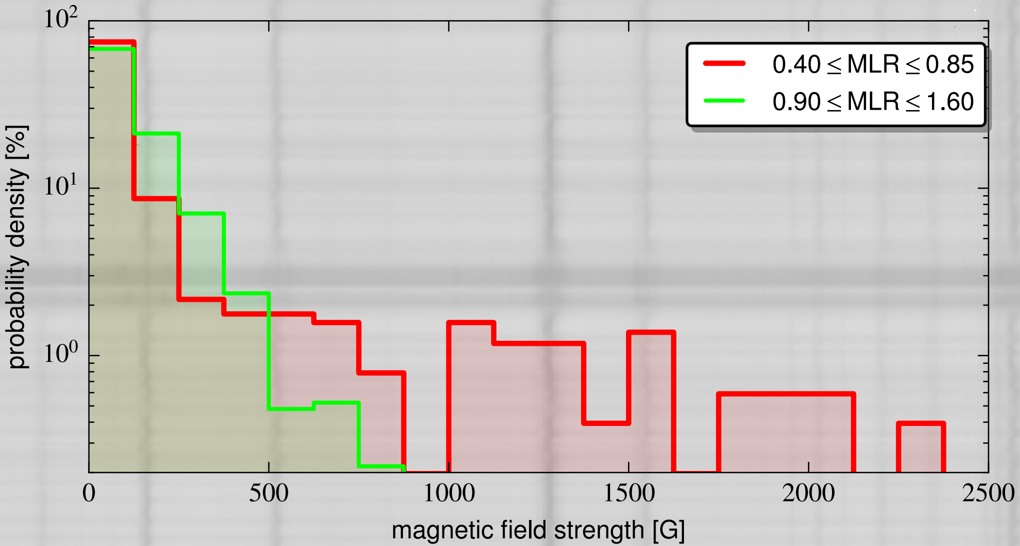

Simple diagnostic techniques: LP/CP - inclination

LP/CP ratio (Solanki et al., 1992)

$$\mathrm{LP/CP} = \frac{\sqrt{Q_{\mathrm{max}}^2 + U_{\mathrm{max}}^2}}{V_{\mathrm{max}}}$$

depends only on γ if

- B sufficiently strong ($\geq$ 1 kG)
- small gradients

depends on γ and B for weaker fields

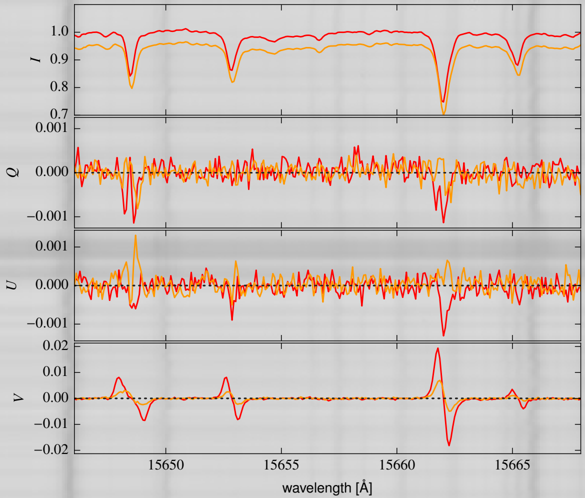

GRIS: LP/CP for Fe I 15648

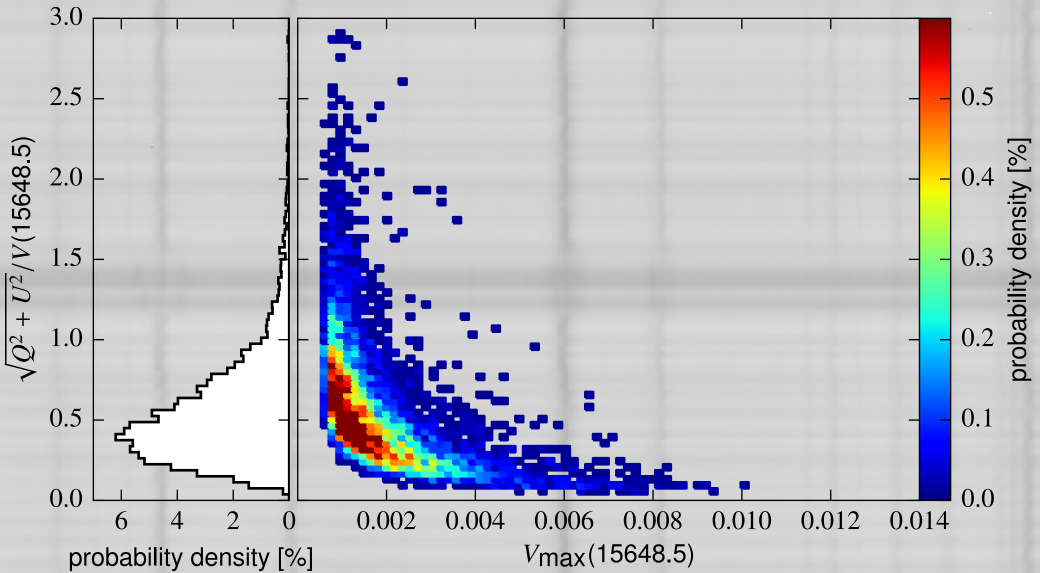

MHD (SSD+IMaX, degraded): LP/CP for Fe I 15648

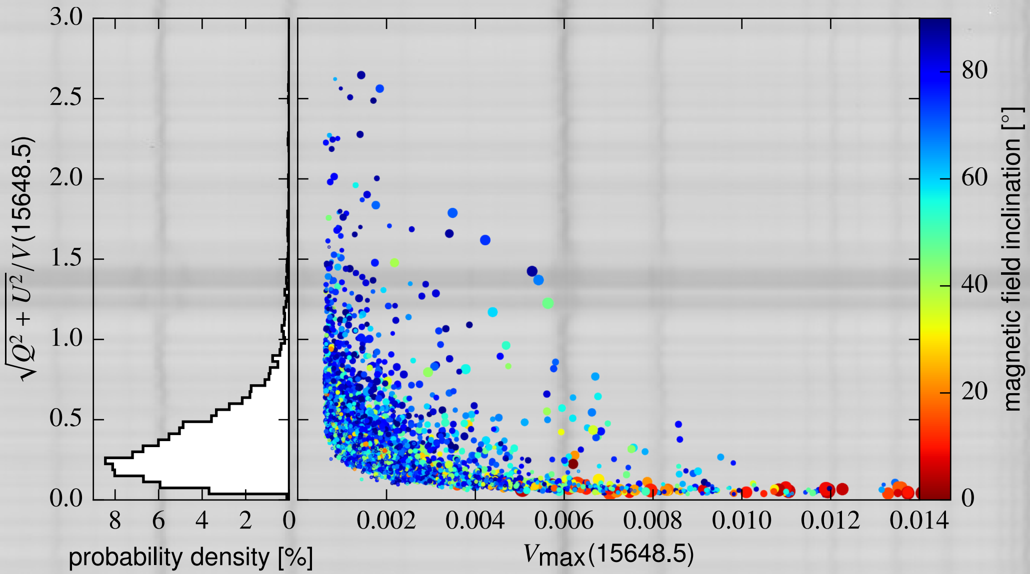

B inclination (SSD + IMaX run)

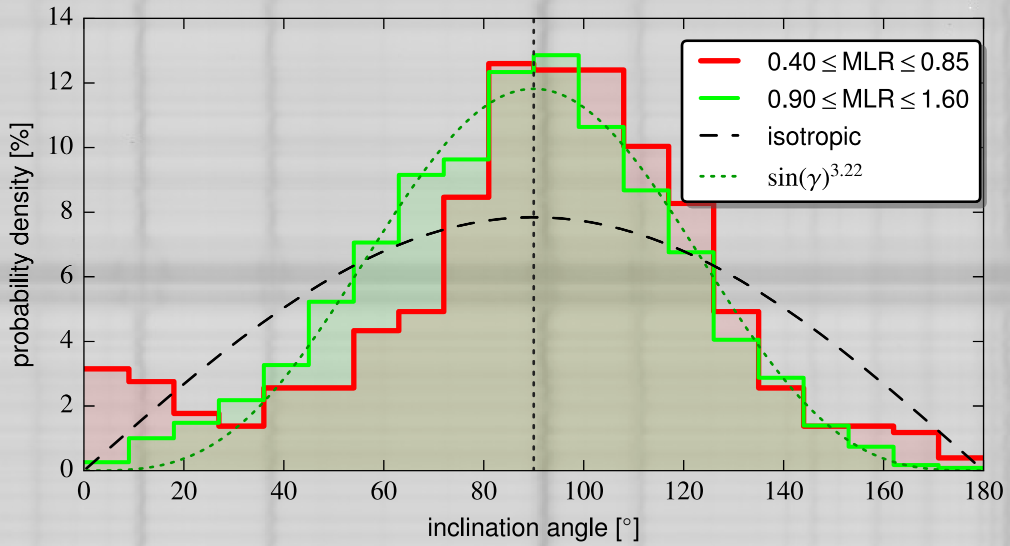

Summary: Quiet Sun Stokes Profiles

Noise Statistics: GRIS$\leftrightarrow$Hinode

- noise level $2.1 \cdot 10^{-4}$ (0.″40)
- TP: $\approx$ 80% above 3σ (cf. Hinode 12.8 s scan: 51%)
- CP: $\approx$ 73% above 3σ (cf. Hinode 12.8 s scan: 49%)
- LP: $\approx$ 40% above 3σ (cf. Hinode 12.8 s scan: 10%)

$\rightarrow$ more reliable inversions are now possible

MLR & LP/CP ratio

MHD-Simul proof:
Good tool to identify kG regions

- some kG patches resolved (vertical fields)
- good agreement with SSD runs
  $\rightarrow$ some kG patches missing
- ”PSF-ring” around kG patches
- hG patches ubiquitous

Proper PSF deconvolution critical for correct interpretation of results!

Bibliography

Asensio Ramos, A. 2009, ApJ, 701, 1032

Asensio Ramos, A. & Martínez González, M. J. 2014, A&A, 572, A98

Asensio Ramos, A. & Trujillo Bueno, J. 2005, ApJL, 635, L109

Asensio Ramos, A., Trujillo Bueno, J., & Landi Degl'Innocenti, E. 2008, ApJ, 683, 542

Berdyugina, S. V. & Fluri, D. M. 2004, A&A, 417, 775

Bommier, V., et al. 2005, A&A, 432, 295

Buehler, D., Lagg, A., & Solanki, S. K. 2013, A&A, 555, A33

Collados, M., et al. 2012, Astronomische Nachrichten, 333, 872

Faurobert, M., et al. 2001, A&A, 378, 627

Faurobert-Scholl, M., et al. 1995, A&A, 298, 289

Kleint, L., et al. 2010, A&A, 524, A37

Lagg, A., et al. 2009, in ASP Conf. Ser., Vol. 415, The Second Hinode Science Meeting: Beyond Discovery-Toward Understanding, ed. Lites, B., et al., 327

Lites, B. W., et al. 2008, ApJ, 672, 1237

Martínez González, M. J., et al. 2008, A&A, 479, 229

Orozco Suárez, D., et al. 2007, Publications of the Astronomical Society of Japan, 59, 837

Rempel, M. 2014, ApJ, 789, 132

Riethmueller, T., et al. 2016, ApJ, in preparation

Schmidt, W., et al. 2012, Astronomische Nachrichten, 333, 796

Shapiro, A. I., et al. 2011, A&A, 529, A139

Shchukina, N. & Trujillo Bueno, J. 2003, in ASP Conf. Ser., Vol. 307, Solar Polarization, ed. Trujillo-Bueno, J. & Sanchez Almeida, J., 336

Solanki, S. K., Rüedi, I. K., & Livingston, W. 1992, A&A, 263, 312

Steiner, O. & Rezaei, R. 2012, in ASP Conf. Ser., Vol. 456, Fifth Hinode Science Meeting, ed. Golub, L., De Moortel, I., & Shimizu, T., 3

Stenflo, J. O. 2010, A&A, 517, A37

Stenflo, J. O. 2013, The Astronomy and Astrophysics Review, 21, 66

Trujillo Bueno, J., Shchukina, N., & Asensio Ramos, A. 2004, Nature, 430, 326

Vögler, A. & Schüssler, M. 2007, A&A, 465, L43

Test using MHD Pore/Plage Run (IMaX)

with PSF

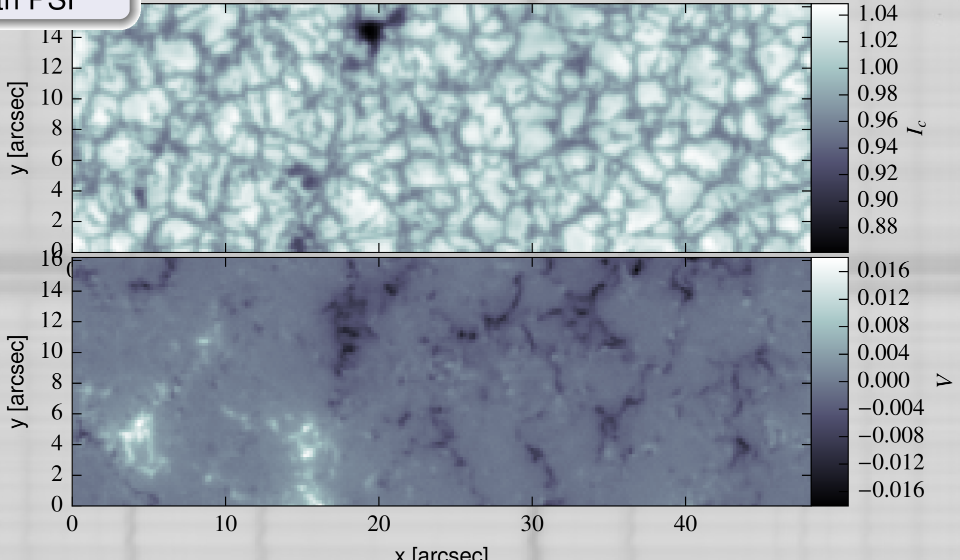

Test using MHD Pore/Plage Run (IMaX)

no PSF

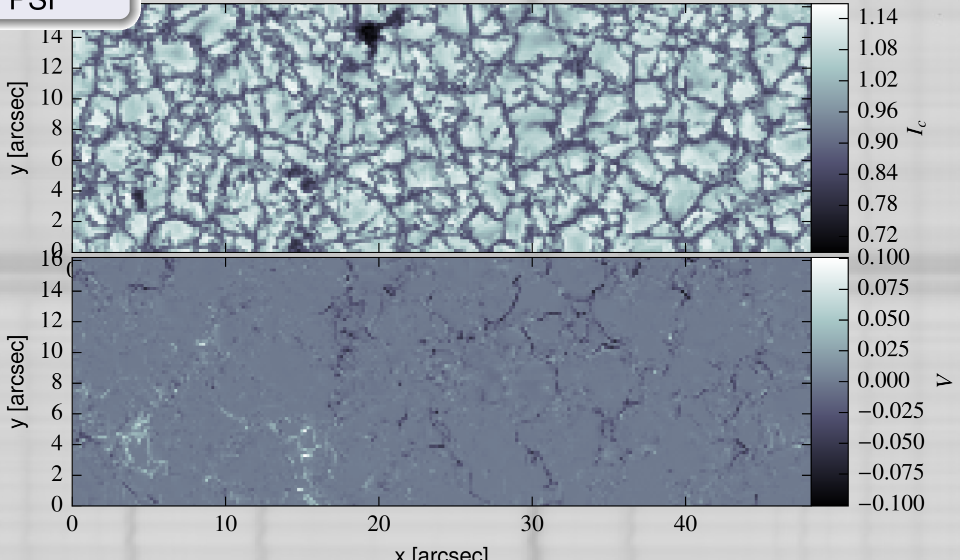

Test using MHD Pore/Plage Run (IMaX)

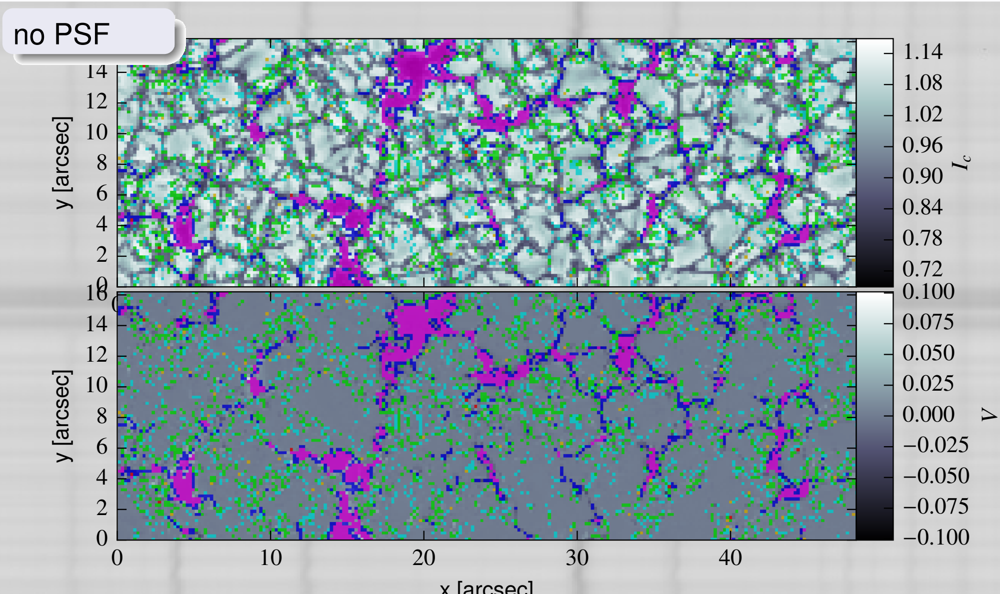

Test using MHD Pore/Plage Run (IMaX)

with PSF

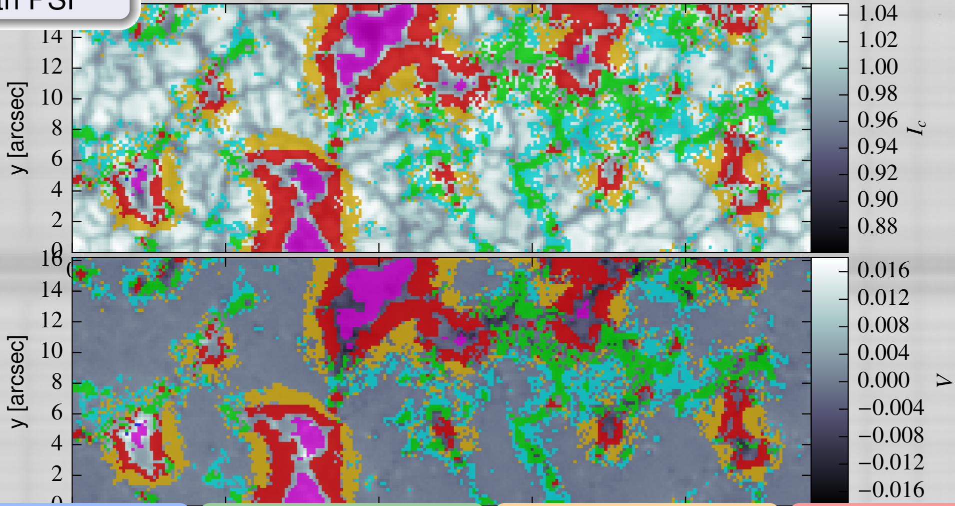

MLR≈1.2, small V_{max} (hG) | MLR≈1.2, large V_{max} (hG) | MLR≈0.6, small V_{max} (kG) | MLR≈0.6, large V_{max} (kG)

Back to GRIS data

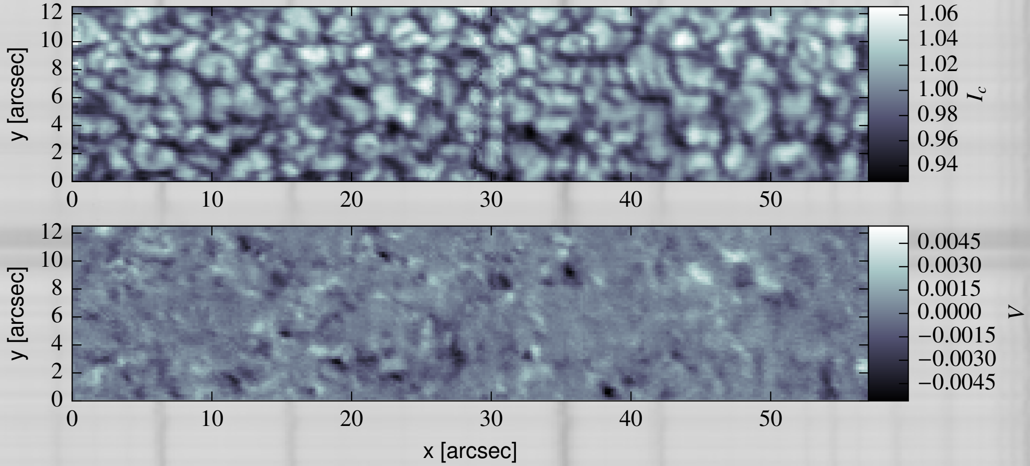

Back to GRIS data

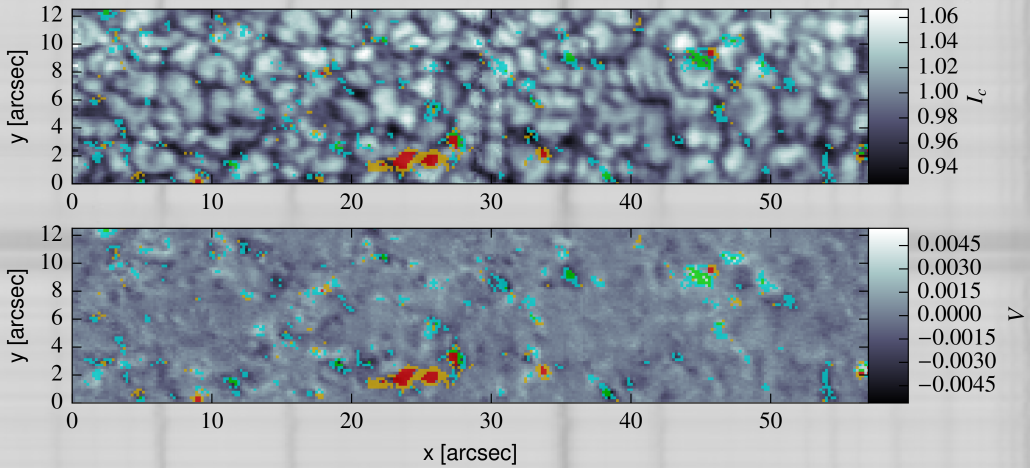

MLR≈1.2, small V_{max} (hG)

MLR≈1.2, large V_{max} (hG)

MLR≈0.6, small V_{max} (kG)

MLR≈0.6, large V_{max} (kG)

Back to GRIS data

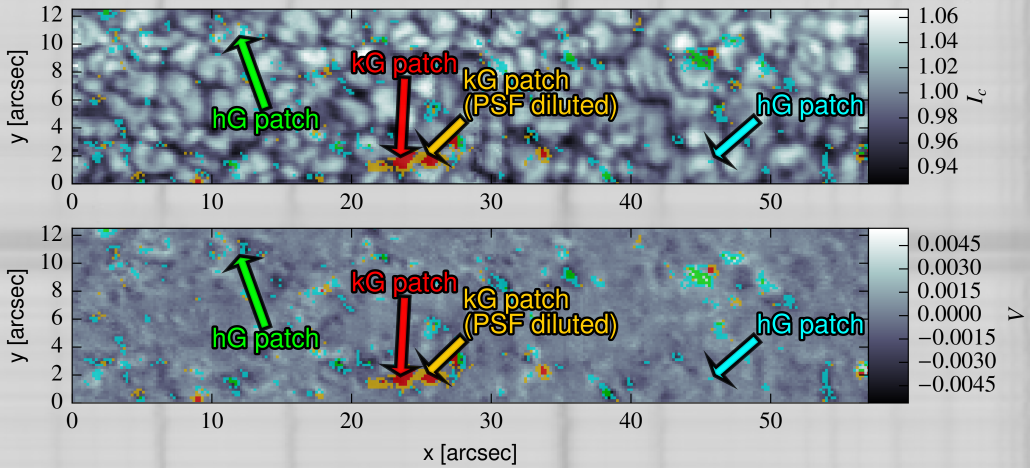

MLR≈1.2, small V_{max} (hG)

MLR≈1.2, large V_{max} (hG)

MLR≈0.6, small V_{max} (kG)

MLR≈0.6, large V_{max} (kG)

MHD (SSD+IMaX, undegraded): LP/CP for Fe I 15648